Parallel Traveling-wave MRI: Antenna Array Approach to Traveling-wave MRI for Parallel Transmission and Acquisition

Y. Pang[1], C. Wang[1], D. Vigneron[1,2], and X. Zhang[1,2]

[1]Radiology and Biomedical imaging, University of California San Francisco, San Francisco, CA, United States, [2]UCSF/UC Berkeley Joint Graduate Group in Bioengineering, San Francisco & Berkeley, CA, United States

Introduction: Recently the traveling-wave [1] has been applied to excite and receive MR signals using patch antenna and waveguide. By utilizing the far field of a single piece patch antenna, homogeneous RF field can be generated to cover samples whose size is larger than the wave length, which is very useful for high field MRI. In this work, we propose a novel design of traveling-wave array which uses patch array to implement multi-source traveling-wave to make parallel transmission and acquisition possible. A 4-element single-feed quadrature transceiver patch array is built as the RF source for 298MHz and a copper bore acts as waveguide. FDTD simulation is performed to evaluate the isolation among array elements, and the RF field distributions on both axial and sagittal planes. G-factor maps for 1D SENSE [2] are calculated on axial planes from 85cm to 135cm away from patch array.

Material and method: As shown in Figure 1a, a copper cylinder bore with 63 cm ID, 65 cm OD and 150 cm length acted as waveguide. On one end of the cylinder bore the 4-element antenna array was built as the source of RF field, as shown in Figure 1b. Each array element was a nearly square ring microstrip patch antenna made from copper foil [3]. The outer dimension of the ring was 12.2 cm by 12 cm, while the inner dimension was a square with 4.4 cm side length. This square slot was carefully cut to reduce resonance frequency of the antenna to 298 MHz. The coaxial feed point was along the diagonal and very close to the square slot, which was able to generate a quadrature RF field [3]. These 4 elements were equispaced (neighboring distance was 8 cm) placed on a piece of TMM 13I material with permittivity of 13.1 and diameter of 63cm. On the back of the substrate the antenna ground was made from a single piece copper foil. The simulation model of this traveling-wave array, the parameters S11 and S21, and the evaluation of RF field distributions were all performed by using the XFDTD6.4 (Remcom Inc.). G-factors for 1D SENSE were calculated using Matlab7.6 (Mathworks Co.).

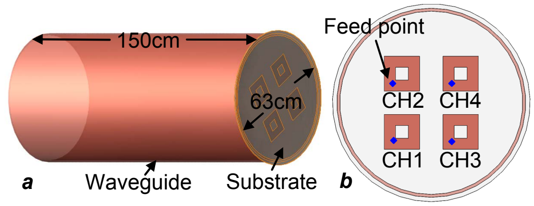

Fig. 1 Traveling-wave array model: (a) copper waveguide; (b) 4-element nearly square ring microstrip patch array acts as RF source.

Results: At 298 MHz the simulated S21, S31 and S41 are all better than -40dB while the S11 is nearly -8 dB. Figure 2 shows the conduction current density (J) on the array surface: when element 1 was fed individually, the currents induced on the other 3 elements are limited, indicating excellent decoupling performance among the elements. When all 4 elements are fed simultaneously, homogeneous B_1 distribution along sagittal plane can be achieved as shown in Figure 3, illustrating "traveling-wave" behavior. Figure 4 shows B_1 profile (combination of x- and y- components) of 4 elements when fed individually. This axial plane is 105cm away from the patch array and the FOV is 61cm. Each element shows different B_1 profile, making it possible to perform parallel transmission and acquisition. At this axial plane the g-factor for 1D SENSE at reduction factor R=2 can reach 1.1. Table 1 shows the g-factor average values at R=2 and 3 for 6 different axial planes from 85cm to 135cm away from the patch array. On each axial plane the FOV is 61cm. Figure 5 shows their corresponding g-factor maps. These data and figures illustrate that parallel imaging can be performed within a large range using the traveling-wave. Furthermore, we also demonstrated that by rotating the element 2 and 3 clockwise 90°, the decoupling can be further improved and the B_1 profiles of the elements are changed, as shown in Figure 6. This provided a simple way to improve the decoupling and manipulate the B_1 profile of each element.

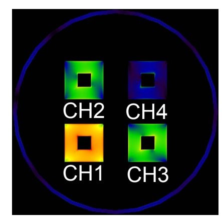

Fig. 2 Conduction current on array surface when only CH1 is fed.

Conclusion and discussion: In this preliminary work a novel design of parallel traveling-wave MRI using single-feed quadrature microstrip patch antenna array has been demonstrated. The transmission coefficients and the conduction current density of each element have demonstrated excellent isolation between array elements. The different sensitivity maps of each element and good g-factor maps at far field make it possible to implement parallel transmission and acquisition using traveling-wave. In in-vivo experiments, it is expected to achieve an even better parallel imaging performance due to the highly asymmetric sensitivity patterns when loaded with high permittivity biological samples [4]. It is also noticed that the orientation and shape of the patch antenna change the sensitivity pattern of each element and decoupling performance.

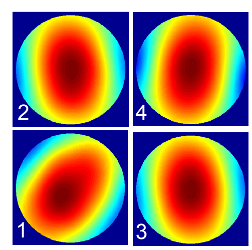

Fig. 4 B_1 patterns of each element of axial plane at 105cm away from the patch array. FOV is 61cm. The number denotes channel number.

References: [1] Brunner DO, et al, Nature 2009; 457: 994-998. [2] Pruessmann KP, et al, MRM 1999; 42: 952-962. [3] Zhang X, et al, ISMRM 2009: p3014. [4] Adriany G, et al, MRM 2005; 53: 434-445.

Acknowledgements: This work was supported in part by NIH grant EB004453 and QB3 opportunity award.

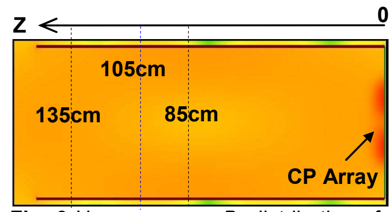

Fig. 3 Homogeneous B_1 distribution of sagittal plane when 4 elements are fed simultaneously.

Position z (cm)	85	95	105	115	125	135
g-factor at R=2	1.25	1.15	1.10	1.13	1.27	1.20
g-factor at R=3	2.80	2.81	2.59	2.52	2.82	2.71

Table 1 G-factors for 1D SENSE at 6 different axial planes (85cm to 135cm away from patch array), with reduction factor of 2 and 3.

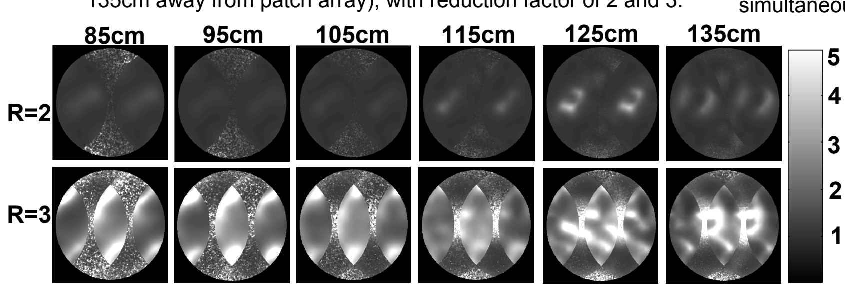

Fig. 5 Corresponding to Table 1, G-factor maps for 1D SENSE at different transverse slices (85cm to 135cm away from patch array), with reduction factor of 2 and 3.

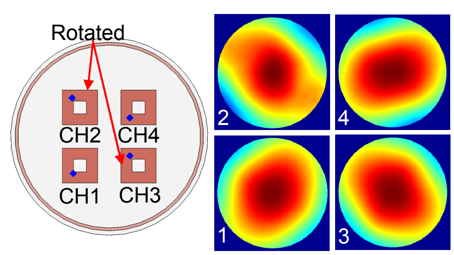

Fig. 6 After rotating the element 2 and 3 clockwise 90°, B_1 profiles of each element at the same axial plane as Fig.4 changes.